

We are IntechOpen, the world's leading publisher of Open Access books Built by scientists, for scientists

4,800

Open access books available

122,000

International authors and editors

135M

Downloads

Our authors are among the

154

Countries delivered to

TOP 1%

most cited scientists

12.2%

Contributors from top 500 universities



WEB OF SCIENCE™

Selection of our books indexed in the Book Citation Index
in Web of Science™ Core Collection (BKCI)

Interested in publishing with us?
Contact book.department@intechopen.com

Numbers displayed above are based on latest data collected.
For more information visit www.intechopen.com



DC/DC Boost-Boost power converter as a didactic system: Experimental results with Matlab/Simulink via current and voltage probes

R. Silva-Ortigoza, M. Antonio-Cruz,
M. Marcelino-Aranda, G. Saldaña-González,
C. A. Merlo-Zapata and P. Pérez-Romero

Additional information is available at the end of the chapter

<http://dx.doi.org/10.5772/58243>

1. Introduction

Great efforts have been made by undergraduate and postgraduate educators in the field of theory validation through experimentation, with the purpose of students gaining better skills during their academic training, motivating the development of didactic prototypes that contribute to this goal. The importance of using such didactic materials can be seen in papers published in journals indexed in Journal Citation Reports [1], the main intention of which is to spread research of this nature, from engineering [2–6] to physics [7, 8].

Theoretical learning about electric circuit analysis at bachelor level, in specialized engineering (such as electronics, electrical, automatic control, bionics, robotics, mechatronics, etc.) and basic sciences (such as physics and mathematics), can be easily grasped by students if they are able to validate this knowledge experimentally. Herein, this fact represents the main motivation for developing a didactic material where power electronics advances are considered, particularly the ones related to the DC/DC Boost-Boost power converter, due to their importance and multiple applications [9–13].

Educational contributions have been reported in the field of analysis, design, modeling, simulation, construction or control of DC/DC power converters as follows. In 2007, Sandoval-Ibarra *et al.* [14] proposed a DC/DC Boost converter design as well as power electronics definitions associated with simple electrical networks. Additionally, in the same year, Sandoval-Ibarra *et al.* [15] introduced an alternative analysis of switched circuits in order to design square wave generators for DC/DC and DC/AC converters. Dudrik and Bauer in 2008 [16] described techniques in the teaching of power electronics converters and devices for undergraduate students through e-learning methods. In 2010, in the

study of Pejović [17], expressions for the discontinuous conduction mode of basic power converters were inferred, relating the output current and output voltage independently to the load type. Likewise, it was mentioned that the method was verified in teaching practice. Campos-Delgado and Espinoza-Trejo in 2010 [18] presented the analysis and construction of the DC/DC Buck, Boost and Buck-Boost power converters. In addition, the design and experimental implementation of proportional integral (PI) controllers for these converters were accomplished. Thus, Altintas in 2011 [19] elaborated an educational graphical user interface (GUI) for the simulation of various topologies of power electronic converters which students can use in order to explore their behavior. The GUI was developed by using Matlab/Simulink, SimPowerSystems, and the GUIDE tool of Matlab, which acts as a front-end that can be used for teaching as well as learning of power converters theory. Also, Abramovitz in 2011 [20] suggested a pedagogical approach to teaching the subject of average modeling of PWM switched-mode power electronics systems through simulation by general-purpose electronic circuit simulators. In 2011, in the work of Deblecker [21] a pre-processing approach was considered. It was based on the $\Sigma - \Delta$ technique for increasing the effective resolution of a digital pulse-width modulator in a voltage-mode controlled Buck converter. Numerical simulations by using Matlab/Simulink allowed the effectiveness of that approach to be verified, and a low-cost development board showed its real behavior. On the other hand, in 2011 Zumel *et al.* [22] designed and implemented, step-by-step, a linear compensator based on a field programmable gate array for a DC/DC Buck power converter. This contribution was oriented to power electronics introductory courses for undergraduate or graduate levels. Recently, in 2012, Liao *et al.* [23] reported a modeling technique for designing switched-mode power supplies (SMPS) aided by Matlab/Simulink. Experimental validation of that technique for the DC/DC Buck power converter, and other SMPS topologies, was realized. Further, in 2012 Lamar *et al.* [24] introduced a problem-based learning method included in a SMPS course, by means of two practical projects: the design and construction of a SMPS prototype (Boost converter), and the static study of a DC/DC power converter topology. Another important contribution that was provided by Silva-Ortigoza *et al.* [25] in 2012 described the model, simulation, construction, and the experimental verifying associated with a DC/DC Boost power converter, as a didactic material intended to support courses on electric circuit analysis. In contrast with this previous work, Choi and Saeedifard [26] in 2012 showed a description of the set of hardware and software tools installed in the power electronics laboratory, constructed at Purdue University, West Lafayette, IN., which was developed primarily to reinforce, experimentally, the fundamental concepts presented in a power electronics course. This facility is used for the design, simulation, control, construction, and verification of power electronic circuits. Finally, work associated with the synthesis or control of DC/DC power converters has been reported [9–11, 27–31].

Having undertaken the educational literature review associated with DC/DC power electronic converters, on the one hand, it was found that the modeling of such converters, generally, was based on equivalent models, validated by specialized software, without deducing the corresponding mathematical models. Also, usually numerical simulations were introduced instead of using experimental implementation. On the other hand, even though the DC/DC power converters, essentially nonlinear, have been controlled via classic control techniques, in the educational literature, generally, modern control techniques have not been proposed for them. For such an aim, the converter models based on state-space

representation is more appropriate as the one to be presented for the Boost-Boost converter in this work.

Thus, the main aim of this work is the modeling, design, simulation, and construction of a prototype associated with a DC/DC Boost-Boost converter to validate its mathematical model, using Kirchhoff current and voltage laws, via experimental tests. This, with the intention of enhancing the acquired theoretical knowledge for students in electric circuit analysis courses. Finally, the simulations are performed using Matlab/Simulink as Simulink provides a graphical environment to the user that facilitates the analysis, design and construction of dynamic systems. Several examples of this software's applications have been presented [9, 11, 19, 21, 23, 26]. Also, books associated with theory, real-world examples, and exercises using either MATLAB or Simulink (MathWorks products) can be found in [32]. On the other hand, the experimental results are obtained using some software tools and laboratory equipment, such as: Matlab/Simulink, a dSPACE DS1104 board [33], current and voltage probes, a power supply, and a function generator.

The work is structured as follows. In Section 2 the mathematical model of the DC/DC Boost-Boost power converter is developed. Matlab/Simulink simulations associated with such a converter are presented in Section 3. The construction of the converter prototype is described in Section 4. Moreover, the experimental validation is developed and analyzed in Section 5. Finally, Section 6 is devoted to the conclusions and future research.

2. Modeling and analysis of a DC/DC Boost-Boost power converter

This section is divided into two parts: the first one deals with the mathematical model deduction via Kirchhoff voltage and current laws for the Boost-Boost power converter, and the second part is related to obtaining the properties of such a converter in steady-state using its average model.

2.1. Boost-Boost power converter modeling

On the one hand, the Boost-Boost converter is composed of two DC/DC Boost power converters connected in cascade. As a consequence, the ideal circuit representation of the DC/DC Boost-Boost power converter, that is, the converter synthesized with switches, is the one shown in Figure 1. On the other hand, herein is presented an alternative circuit representation for the converter under study, using MOSFET transistors as switches, as shown in Figure 2.

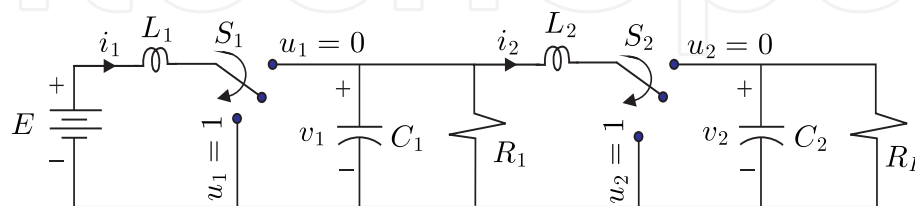


Figure 1. DC/DC Boost-Boost power converter ideal circuit.

In the system shown in Figure 1, inputs u_1 and u_2 can take values in the discrete set $\{0, 1\}$, corresponding to the positions of the switches S_1 and S_2 , respectively. These positions are set in practice by using transistors (Q_1 and Q_2) in on/off operating mode. The transistors in

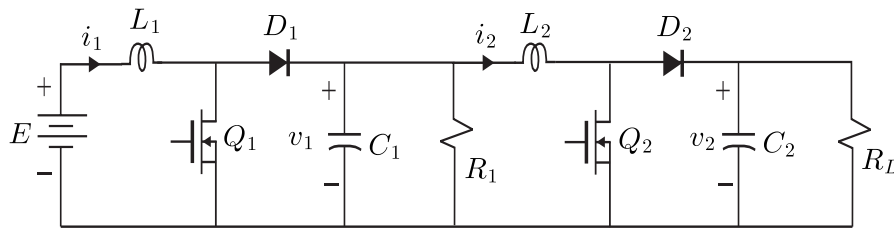


Figure 2. DC/DC Boost-Boost power converter circuit implemented with transistors.

the on-state are equivalent to the positions $u_1 = 1$ and $u_2 = 1$, and the off-states correspond to the positions $u_1 = 0$ and $u_2 = 0$. In the derivation of the mathematical model for the converter it is assumed that the circuit operates in continuous conduction mode, that is, the average value of the inductors currents are never lower than zero [29]. The variables i_1 , v_1 , i_2 , and v_2 correspond to the currents and voltages associated to L_1 , C_1 , L_2 , and C_2 , respectively. The loads are represented by R_1 and R_L , which correspond to each output stage of the Boost converters that compose the Boost-Boost converter. Finally, E denotes the power converter primary supply source.

An important feature of the Boost-Boost converter output voltage v_2 , is that it satisfies the following condition:

$$v_2 \geq E,$$

which can be shown by analyzing such a converter in steady-state. This is the reason why this converter is also known as a double step-up converter.

From Figure 1 and the Kirchhoff voltage and current laws (abbreviated to KVL and KCL, respectively), the switched model, which describes the Boost-Boost converter dynamic evolution, is obtained as follows.

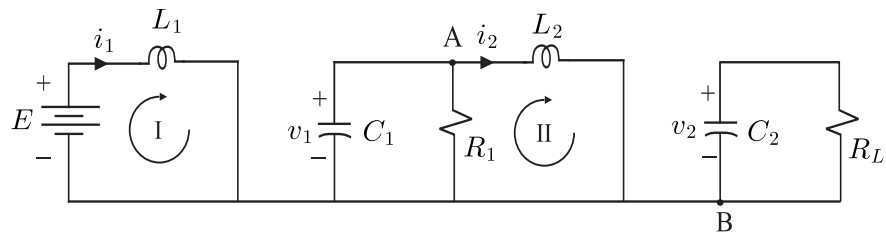
- 1/2. –The on/off states of transistors Q_1 and Q_2 are considered to generate the four equivalent circuits shown in Figure 3, each circuit is represented by a fourth-order-differential equations subsystem. Thus, four mathematical subsystems are generated.
- 2/2. –These four subsystems are integrated only in a system of fourth-order differential equations, which describes the converter's nonlinear dynamics.

The aforementioned process is accomplished as follows:

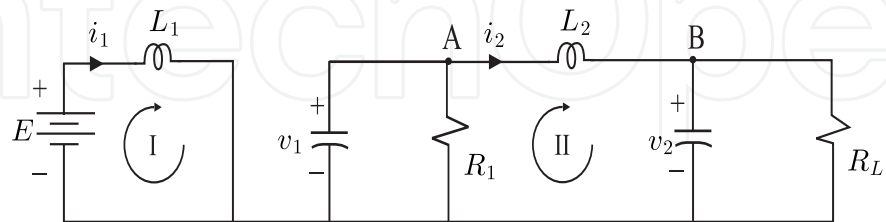
- a) *Equivalent Circuit I* occurs when transistors Q_1 and Q_2 conduct, that is, $u_1 = 1$ and $u_2 = 1$, and diodes D_1 and D_2 are reverse biased. Then, the equivalent circuit is shown in Figure 3(a). Applying KVL to meshes I and II, the following equations for the currents i_1 and i_2 , respectively, are obtained:

$$L_1 \frac{di_1}{dt} = E, \quad (1)$$

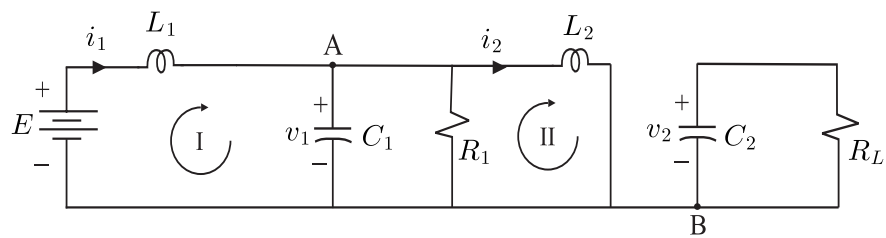
$$L_2 \frac{di_2}{dt} = v_1. \quad (2)$$



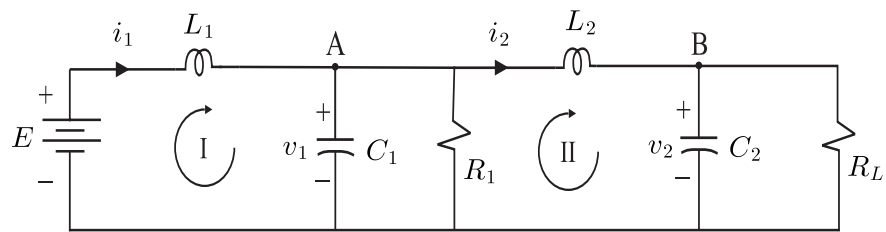
(a) Equivalent circuit I: $u_1 = 1$ and $u_2 = 1$.



(b) Equivalent circuit II: $u_1 = 1$ and $u_2 = 0$.



(c) Equivalent circuit III: $u_1 = 0$ and $u_2 = 1$.



(d) Equivalent circuit IV: $u_1 = 0$ and $u_2 = 0$.

Figure 3. DC/DC Boost-Boost power converter operating modes.

Moreover, applying KCL for nodes A and B in Figure 3(a), the differential equations related to voltages v_1 and v_2 are obtained by

$$C_1 \frac{dv_1}{dt} = -\frac{v_1}{R_1} - i_2, \quad (3)$$

$$C_2 \frac{dv_2}{dt} = -\frac{v_2}{R_L}. \quad (4)$$

- b) *Equivalent circuit II* is generated when Q_1 conducts and Q_2 does not conduct, that is, $u_1 = 1$ and $u_2 = 0$, then the diode D_1 is reverse biased and diode D_2 is forward biased. Thus, the corresponding equivalent circuit is shown in Figure 3(b). Applying KVL to

meshes I and II the equations for i_1 and i_2 , respectively, are obtained:

$$L_1 \frac{di_1}{dt} = E, \quad (5)$$

$$L_2 \frac{di_2}{dt} = v_1 - v_2. \quad (6)$$

Applying KCL to nodes A and B in Figure 3(b), the dynamics associated to v_1 and v_2 , respectively, are obtained:

$$C_1 \frac{dv_1}{dt} = -\frac{v_1}{R_1} - i_2, \quad (7)$$

$$C_2 \frac{dv_2}{dt} = i_2 - \frac{v_2}{R_L}. \quad (8)$$

- c) *Equivalent circuit III* is presented when Q_1 does not conduct and Q_2 conducts, that is, $u_1 = 0$ and $u_2 = 1$, D_1 is forward biased and D_2 is reverse biased. Then, the resultant circuit is as shown in Figure 3(c). Applying KVL to meshes I and II, and the KCL to nodes A and B in Figure 3(c), the equations for i_1 , i_2 , v_1 , and v_2 , respectively, are obtained:

$$L_1 \frac{di_1}{dt} = -v_1 + E, \quad (9)$$

$$L_2 \frac{di_2}{dt} = v_1, \quad (10)$$

$$C_1 \frac{dv_1}{dt} = i_1 - \frac{v_1}{R_1} - i_2, \quad (11)$$

$$C_2 \frac{dv_2}{dt} = -\frac{v_2}{R_L}. \quad (12)$$

- d) *Equivalent circuit IV* occurs when transistors Q_1 and Q_2 do not conduct, that is, $u_1 = 0$ and $u_2 = 0$, D_1 and D_2 are forward biased. The equivalent circuit is shown in Figure 3(d). In order to achieve the equations that govern i_1 , i_2 , v_1 , and v_2 , KVL and KCL are applied, obtaining the following:

$$L_1 \frac{di_1}{dt} = -v_1 + E, \quad (13)$$

$$L_2 \frac{di_2}{dt} = v_1 - v_2, \quad (14)$$

$$C_1 \frac{dv_1}{dt} = i_1 - \frac{v_1}{R_1} - i_2, \quad (15)$$

$$C_2 \frac{dv_2}{dt} = i_2 - \frac{v_2}{R_L}. \quad (16)$$

Equations related to i_1 , (1), (5), (9), and (13), can be associated, using u_1 , producing (17). The dynamics associated with v_1 is obtained from a combination of (3), (7), (11), and (15) through u_1 , generating (18). The unification of (2), (6), (10), and (14) through u_2 , produces the dynamics associated to i_2 , determined by (19). Following a similar process for v_2 , associating (4), (8), (12), and (16), (20) is produced. Thus, the Boost-Boost converter dynamics is determined by the following nonlinear differential equations system:

$$L_1 \frac{di_1}{dt} = -(1 - u_1) v_1 + E, \quad (17)$$

$$C_1 \frac{dv_1}{dt} = (1 - u_1) i_1 - \frac{v_1}{R_1} - i_2, \quad (18)$$

$$L_2 \frac{di_2}{dt} = v_1 - (1 - u_2) v_2, \quad (19)$$

$$C_2 \frac{dv_2}{dt} = (1 - u_2) i_2 - \frac{v_2}{R_L}. \quad (20)$$

This is called the converter *switched model* referring to the binary values associated with the switches positions, that is, $u_1 \in \{0, 1\}$ and $u_2 \in \{0, 1\}$.

2.2. Converter steady-state analysis

In order to know the Boost-Boost converter properties in steady-state its average model is used [11], which is determined by

$$L_1 \frac{di_1}{dt} = -(1 - u_{1av}) v_1 + E, \quad (21)$$

$$C_1 \frac{dv_1}{dt} = (1 - u_{1av}) i_1 - \frac{v_1}{R_1} - i_2, \quad (22)$$

$$L_2 \frac{di_2}{dt} = v_1 - (1 - u_{2av}) v_2, \quad (23)$$

$$C_2 \frac{dv_2}{dt} = (1 - u_{2av}) i_2 - \frac{v_2}{R_L}, \quad (24)$$

where i_1 , v_1 , i_2 , and v_2 now denote average currents and voltages associated with L_1 , C_1 , L_2 , and C_2 , respectively, whereas u_{1av} and u_{2av} represent average position functions of the switches or duty cycles [9, 29], taking values in the interval $[0, 1)$.

No distinction is made between the variables of the average model (21)–(24) and the switched model (17)–(20). However, in order to distinguish one model from the other, the inputs to the average model are denoted by u_{1av} and u_{2av} , and the inputs of the switched model are denoted by u_1 and u_2 . This difference is used in the rest of the work. Furthermore, it is important to note that theoretical justification of the average models has been extensively dealt with since the beginning of power electronics [27].

Based on the average model (21)–(24), the evaluation of the converter equilibrium point proceeded, denoted by $(\bar{i}_1, \bar{v}_1, \bar{i}_2, \bar{v}_2)$, that is, the values of $i_1, v_1, i_2,$ and v_2 in steady-state as a response to the constant average inputs \bar{u}_{1av} and \bar{u}_{2av} . Thus, (21)–(24) in equilibrium satisfies the following algebraic equations system:

$$0 = -(1 - \bar{u}_{1av}) \bar{v}_1 + E, \quad (25)$$

$$0 = (1 - \bar{u}_{1av}) \bar{i}_1 - \frac{\bar{v}_1}{R_1} - \bar{i}_2, \quad (26)$$

$$0 = \bar{v}_1 - (1 - \bar{u}_{2av}) \bar{v}_2, \quad (27)$$

$$0 = (1 - \bar{u}_{2av}) \bar{i}_2 - \frac{\bar{v}_2}{R_L}, \quad (28)$$

which is represented as a matrix equation by

$$\begin{bmatrix} 0 & -(1 - \bar{u}_{1av}) & 0 & 0 \\ (1 - \bar{u}_{1av}) & -\frac{1}{R_1} & -1 & 0 \\ 0 & 1 & 0 & -(1 - \bar{u}_{2av}) \\ 0 & 0 & (1 - \bar{u}_{2av}) & -\frac{1}{R_L} \end{bmatrix} \begin{bmatrix} \bar{i}_1 \\ \bar{v}_1 \\ \bar{i}_2 \\ \bar{v}_2 \end{bmatrix} = \begin{bmatrix} -E \\ 0 \\ 0 \\ 0 \end{bmatrix}. \quad (29)$$

By solving (29) for $\bar{i}_1, \bar{v}_1, \bar{i}_2,$ and \bar{v}_2 the following is obtained:

$$\begin{bmatrix} \bar{i}_1 \\ \bar{v}_1 \\ \bar{i}_2 \\ \bar{v}_2 \end{bmatrix} = \begin{bmatrix} \frac{E}{R_1 R_L} \frac{R_1 + R_L (1 - \bar{u}_{2av})^2}{(1 - \bar{u}_{1av})^2 (1 - \bar{u}_{2av})^2} \\ \frac{E}{1 - \bar{u}_{1av}} \\ \frac{E}{R_L} \frac{1}{(1 - \bar{u}_{1av})(1 - \bar{u}_{2av})^2} \\ \frac{E}{(1 - \bar{u}_{1av})(1 - \bar{u}_{2av})} \end{bmatrix}. \quad (30)$$

Therefore, (30) provides the average value of the variables $i_1, v_1, i_2,$ and v_2 in steady-state. Furthermore, from the relation of \bar{v}_2 with \bar{u}_{1av} and \bar{u}_{2av} it can be seen that the output of this converter satisfies the inequality $\bar{v}_2 \geq E$, as initially stated, since \bar{u}_{1av} and $\bar{u}_{2av} \in [0, 1)$.

3. Converter numerical simulations with Matlab/Simulink

In this section, numerical simulations of the Boost-Boost converter switched model (17)–(20) are performed, by using Matlab/Simulink. This will enable the dynamic evolution of the system variables $i_1, v_1, i_2,$ and v_2 to be known in response to different switched inputs u_1 and u_2 , generated via the constant average inputs \bar{u}_{1av} and \bar{u}_{2av} belonging to the interval $[0, 1)$.

3.1. Simulink blocks for simulations

The developed diagram for the converter's numerical simulations consists of three blocks, namely, *inputs*, *Boost-Boost system*, and *outputs*, (see Figure 4). The description associated with the block diagram shown in the Figure 4 is as follows:

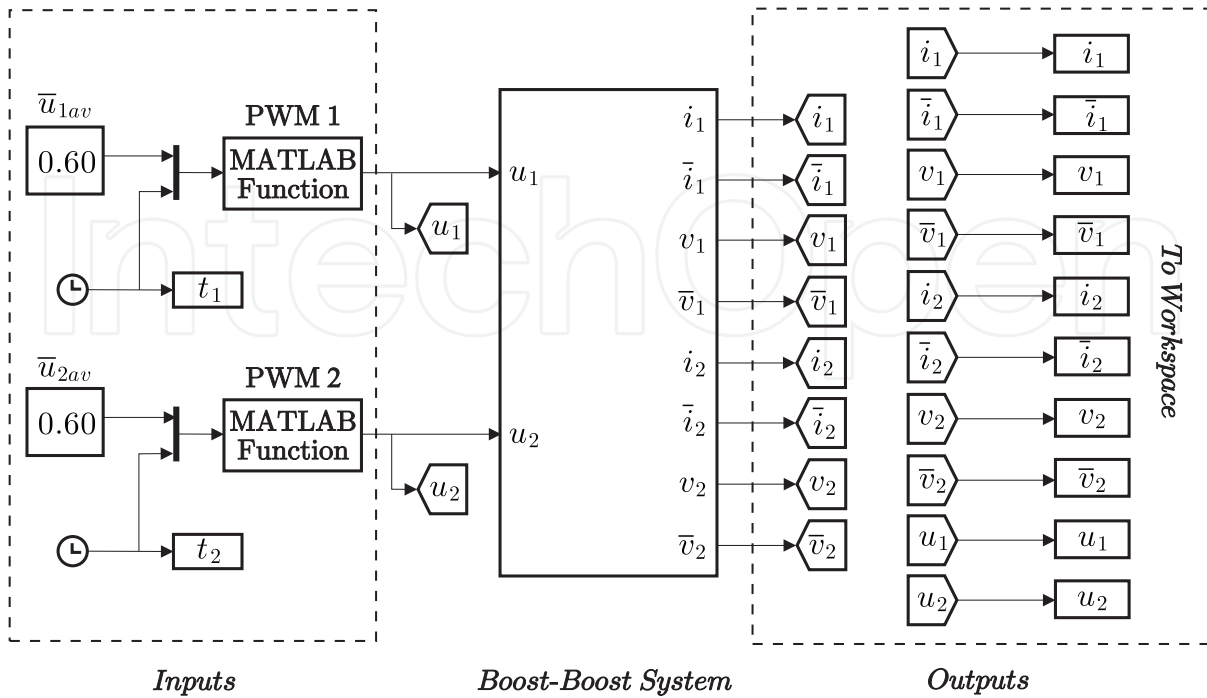


Figure 4. Diagram developed in Matlab/Simulink to perform simulations.

- Inputs.** The inputs associated with this block correspond to the constant average values \bar{u}_{1av} and \bar{u}_{2av} , which represent the inputs to blocks PWM1 and PWM2. Each PWM block is constructed with a Matlab embedded function [34], the outputs of which deliver the switched signals u_1 and u_2 , respectively. The code associated with the block PWM1 or block PWM2 is shown in Table 1.

```

function sal=DUTY_CYCLE(uav1)
ciclo=uav1(1);
t=uav1(2);
A=1;
fp=50000;
u1=A*((square(2*pi*fp*t,ciclo)+1)/2);
sal=u1;
    
```

Table 1. Code for the block PWM1 or block PWM2.

- Boost-Boost system.** In this block the switched model (17)–(20) is programmed. For this purpose an embedded function of Matlab is used (see Figure 5), whereas, the code associated with this function is presented in Table 2.
- Outputs.** This block delivers the dynamic evolution of the variables i_1 , v_1 , i_2 , and v_2 and the values in steady-state \bar{i}_1 , \bar{v}_1 , \bar{i}_2 , and \bar{v}_2 , respectively, obtained via simulation.

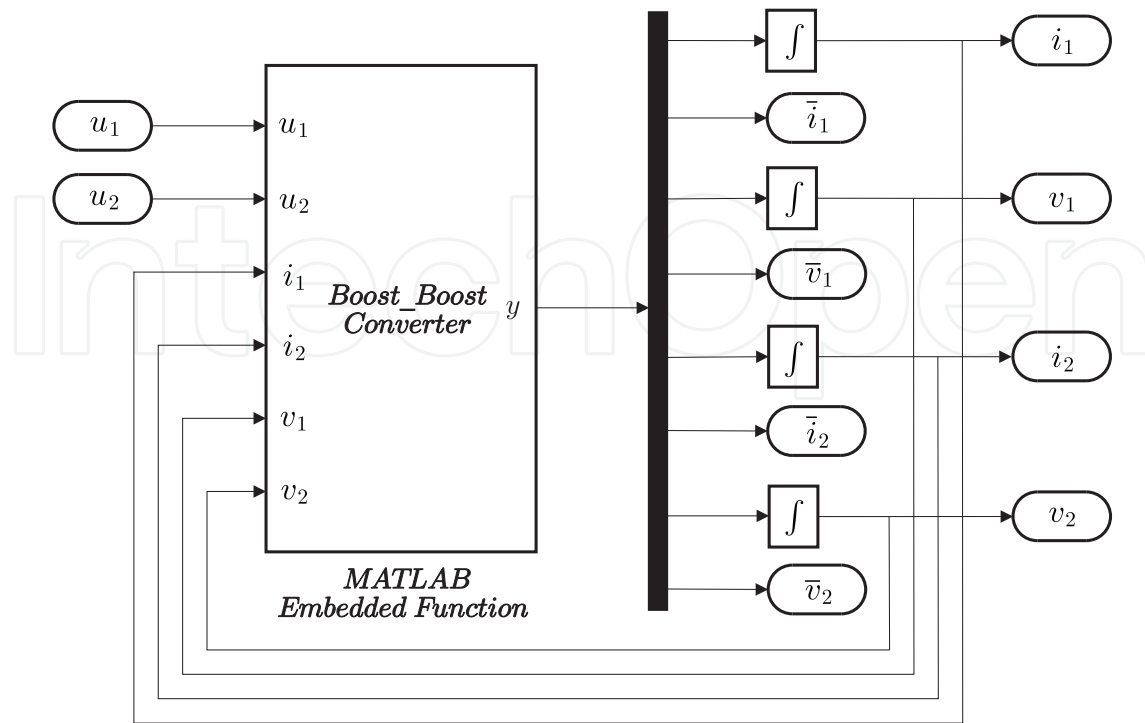


Figure 5. Block *Boost-Boost* system.

```
function y=Boost_Boost(u1,u2,i1,i2,v1,v2)
E=12;L1=4.94e-3;C1=12.2e-6;L2=3e-3;C2=12.2e-6;R1=474;
RL=275;a1=0.55;a2=0.55;
di1=(-(1-u1)*(v1/L1))+(E/L1);
dv1=((1-u1)*(i1/C1))-(v1/(R1*C1))-(i2/C1);
di2=(v1/L2)-((1-u2)*(v2/L2));
dv2=((1-u2)*(i2/C2))-(v2/(RL*C2));
v1d=(E/(1-a1));
i1d=((E/(R1*RL))*((R1+((RL)*((1-a2)^2)))/(((1-a1)^2)*((1-a2)^2)));
v2d=(E/((1-a1)*(1-a2)));
i2d=((E/RL)*(1/((1-a1)*((1-a2)^2))));
y=[di1;dv1;di2;dv2];
```

Table 2. *Boost-Boost* system code.

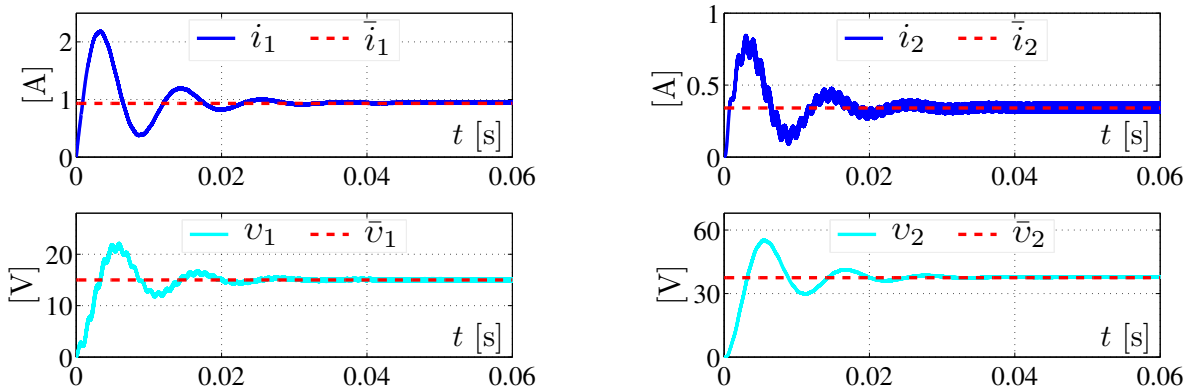
3.2. Simulation results

In the numerical simulations implementation, the following values for the parameters associated with (17)–(20) were considered:

$$L_1 = 4.94 \text{ mH}, C_1 = 12.2 \text{ } \mu\text{F}, L_2 = 3 \text{ mH}, C_2 = 12.2 \text{ } \mu\text{F}, R_1 = 474 \text{ } \Omega, R_L = 275 \text{ } \Omega,$$

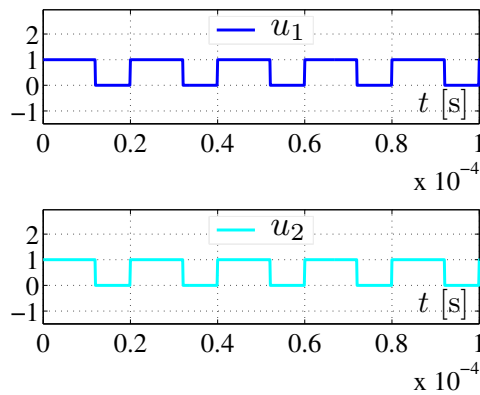
for the cases in which E takes values of 6 V and 12 V, respectively. The justification of the parameters is shown in next section, whereas, the simulation results associated with the converter under study are presented as follows:

- *Simulation I* considers that $E = 6$ V and the system inputs take the average values $\bar{u}_{1av} = 0.60$ and $\bar{u}_{2av} = 0.60$. In steady-state, according to (30), $(\bar{i}_1, \bar{v}_1, \bar{i}_2, \bar{v}_2) = (931 \text{ mA}, 15 \text{ V}, 340 \text{ mA}, 37.5 \text{ V})$. For this case, the simulation results are shown in Figure 6.
- *Simulation II* considers that $E = 12$ V and the inputs are $\bar{u}_{1av} = 0.55$ and $\bar{u}_{2av} = 0.55$. According to (30) it is found that $(\bar{i}_1, \bar{v}_1, \bar{i}_2, \bar{v}_2) = (1.19 \text{ A}, 26.67 \text{ V}, 480 \text{ mA}, 59.26 \text{ V})$. The corresponding simulation results can be seen in Figure 7.



(a) Current through the inductor L_1 and voltage at capacitor C_1 .

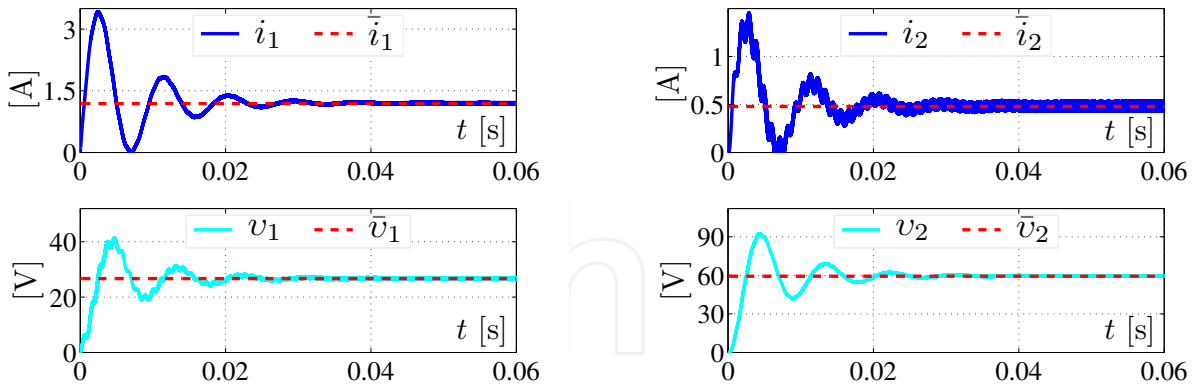
(b) Current through the inductor L_2 and voltage at capacitor C_2 .



(c) Inputs $u_1 = 60\%$ and $u_2 = 60\%$.

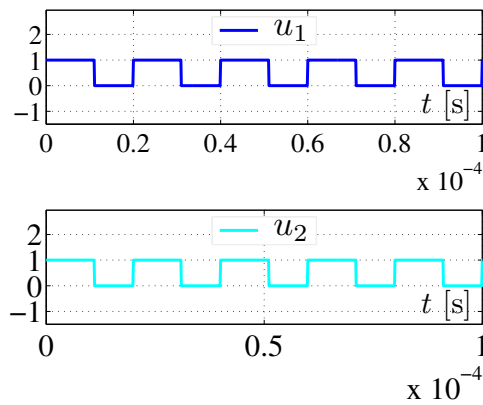
Figure 6. Dynamic response obtained from *simulation I*.

It can be observed that the simulation results validate the converter mathematical model and that the steady-state values of the system variables behave according to (30). Also, it was verified that this converter operates as a voltage amplifier with respect to E , when $u_{1av} \in (0, 1)$ and $u_{2av} \in (0, 1)$.



(a) Current through the inductor L_1 and voltage at capacitor C_1 .

(b) Current through the inductor L_2 and voltage at capacitor C_2 .



(c) Inputs $u_1 = 55\%$ and $u_2 = 55\%$.

Figure 7. Dynamic response obtained from simulation II.

4. Boost-Boost power converter construction

In this section, first the process followed to obtain the design parameters of the DC/DC Boost-Boost power converter is described. Subsequently, the construction of such a converter is presented.

4.1. Boost-Boost power converter design

Table 3 shows the design specifications for the converter construction. Two cases are considered: the first refers to $E = 6$ V and the second to $E = 12$ V.

Here, calculations corresponding to the first case are presented. According to (30) and the converter design specification, the average inputs \bar{u}_{1av} and \bar{u}_{2av} are defined by

$$\bar{u}_{1av} = 1 - \frac{E}{\bar{v}_1} = 1 - \frac{6 \text{ V}}{20 \text{ V}} = 0.70,$$

$$\bar{u}_{2av} = 1 - \frac{E}{(1 - \bar{u}_{1av})\bar{v}_2} = 1 - \frac{6 \text{ V}}{(1 - 0.70)(66.67) \text{ V}} \approx 0.70.$$

	Case 1	Case 2
Input voltage (E)	6 V	12 V
Output voltages (\bar{v}_1 and \bar{v}_2)	$\bar{v}_1 = 20$ V $\bar{v}_2 = 66.67$ V	$\bar{v}_1 = 26.67$ V $\bar{v}_2 = 59.26$ V
Output power associated to R_1 (P_{R_1}) and R_L (P_{R_L})	$P_{R_1} = 0.85$ W $P_{R_L} = 16$ W	$P_{R_1} = 1.48$ W $P_{R_L} = 12.19$ W
Switching frequency (f)	50 kHz	50 kHz
Current ripple ($\Delta \bar{i}_1$ and $\Delta \bar{i}_2$)	5% of nominal value for \bar{i}_1 , and 12% of nominal value for \bar{i}_2	
Voltage ripple ($\Delta \bar{v}_1$ and $\Delta \bar{v}_2$)	5% of nominal value for \bar{v}_1 and \bar{v}_2	

Table 3. Design specifications for the Boost-Boost converter.

Since the desired power in load resistance R_1 is 0.85 W, with a voltage of 20 V, then R_1 is calculated using the expression $R_1 = \frac{\bar{v}_1^2}{P_{R_1}}$, which produces $R_1 \approx 470.59 \Omega$. Similarly, if $P_{R_L} = 16$ W and $\bar{v}_2 = 66.67$ V, then the load resistance $R_L \approx 277.81 \Omega$. On the other hand, the current \bar{i}_{R_1} flowing through R_1 is calculated from the expression $\bar{i}_{R_1} = \frac{P_{R_1}}{\bar{v}_1} = 42.5$ mA, whereas the current through R_L is defined by $\bar{i}_{R_L} = \frac{P_{R_L}}{\bar{v}_2} \approx 240$ mA. Moreover, according to (30) the currents through the inductors, L_1 and L_2 , are $\bar{i}_1 \approx 2.81$ A and $\bar{i}_2 \approx 800$ mA, respectively.

In the calculations of the inductance and capacitance minimum values associated with the first stage, in order to satisfy the converter design specifications, the following relations are employed [35]:

$$L_{1 \min} = \frac{E \bar{u}_{1av}}{f \Delta \bar{i}_1} = \frac{(6 \text{ V}) (0.70)}{(50 \text{ kHz}) (0.05) (2.81 \text{ A})} \approx 0.60 \text{ mH}, \quad (31)$$

$$C_{1 \min} = \frac{\bar{u}_{1av}}{R_1 f \Delta \bar{v}_1} \bar{v}_1 = \frac{(0.70)}{(470.59 \Omega) (50 \text{ kHz}) (0.05) (20 \text{ V})} (20 \text{ V}) \approx 0.59 \mu\text{F}. \quad (32)$$

Furthermore, according to [35] the condition $T \ll 2R_1C_1$ must be satisfied, where $T = 1/f$, which is achieved when $C_{1 \min}$ is multiplied by 20, generating that C_1 is determined by

$$C_1 = 11.8 \mu\text{F}.$$

Now, the minimum values for inductance and capacitance of the second stage can be calculated as follows:

$$L_{2 \min} = \frac{\bar{v}_1 \bar{u}_{2av}}{f \Delta \bar{i}_2} = \frac{(20 \text{ V}) (0.70)}{(50 \text{ kHz}) (0.12) (0.80 \text{ A})} \approx 2.92 \text{ mH}, \quad (33)$$

$$C_{2\min} = \frac{\bar{u}_{2av}}{R_L f \Delta \bar{v}_2} \bar{v}_2 = \frac{(0.70)}{(277.81 \Omega) (50 \text{ kHz}) (0.05) (66.67 \text{ V})} (66.67 \text{ V}) \approx 1.01 \mu\text{F}. \quad (34)$$

Condition $T \ll 2R_2C_2$, can be satisfied multiplying $C_{2\min}$ by 12 generating the following:

$$C_2 = 12.12 \mu\text{F}.$$

Finally, the commercial values employed for the converter components were the following:

$$\begin{aligned} L_1 &= 4.94 \text{ mH}, C_1 = 12.2 \mu\text{F}, L_2 = 3 \text{ mH}, \\ C_2 &= 12.2 \mu\text{F}, R_1 = 474 \Omega/50 \text{ W}, R_L = 275 \Omega/50 \text{ W}. \end{aligned} \quad (35)$$

The inductors were built on a ETD49/25/16 core with 3C85 material from Ferroxcube. They were used 110 and 69 turns of 18.5 AWG Litz wire for L_1 and L_2 , respectively, with 175 strands. The L_1 internal series resistance, R_{s1} , has associated 10.5Ω , while the L_2 internal series resistance, R_{s2} , 6.6Ω . Furthermore, the C_1 and C_2 values were obtained by connecting two MKP capacitors from Kemet in parallel: one of $10 \mu\text{F}$ and another one of $2 \mu\text{F}$, both rated at 275 V.

Following a similar procedure as the one aforementioned, we have found that approach values for L_1 , C_1 , L_2 , C_2 , R_1 , and R_L , as they are shown in (35), are required for *Case 2* presented in Table 3.

4.2. Experimental prototype

Figure 8 shows the electronic diagram proposed for the Boost-Boost converter, which is composed of two blocks, namely, *Boost-Boost converter* and *function generator*. The description associated with these blocks is presented as follows:

- *Boost-Boost converter*. Figure 8 shows how the variables i_1 , v_1 , i_2 , and v_2 , are measured. In order to visualize the converter dynamic response Matlab/Simulink and a DS1104 electronic board from dSPACE are employed, along with two Tektronix A622 AC/DC current probes (for i_1 and i_2), and two Tektronix P6139A voltage probes (for v_1 and v_2), whereas, a BK Precision 1795 DC power supply is used to provide E .
- *Function generator*. This block is implemented using an HP 8111A function generator, which possesses an option to set the pulse width, to produce the input signals u_1 and u_2 with a 5 V amplitude, which is an appropriate voltage level to trigger the NTE2984 transistors. These transistors have a logic level gate and operate at high speed. Some important parameters of this device are the following: drain–source breakdown voltage $BV_{DSS} = 60 \text{ V}$, absolute maximum drain current $I_D = 17 \text{ A}$ with continuous $V_{GS} = 5 \text{ V}$ to $25 \text{ }^\circ\text{C}$, rise time $t_r = 110 \text{ ns}$, fall time $t_f = 41 \text{ ns}$, turn-on delay time $t_{d(\text{on})} = 11 \text{ ns}$, turn-off delay time $t_{d(\text{off})} = 23 \text{ ns}$, static drain–source on resistance $R_{DS(\text{on})} = 0.14 \Omega$ and the maximum operating temperature is $175 \text{ }^\circ\text{C}$. The visualizing of u_1 and u_2 are accomplished with a Tektronic TDS 3034B oscilloscope.

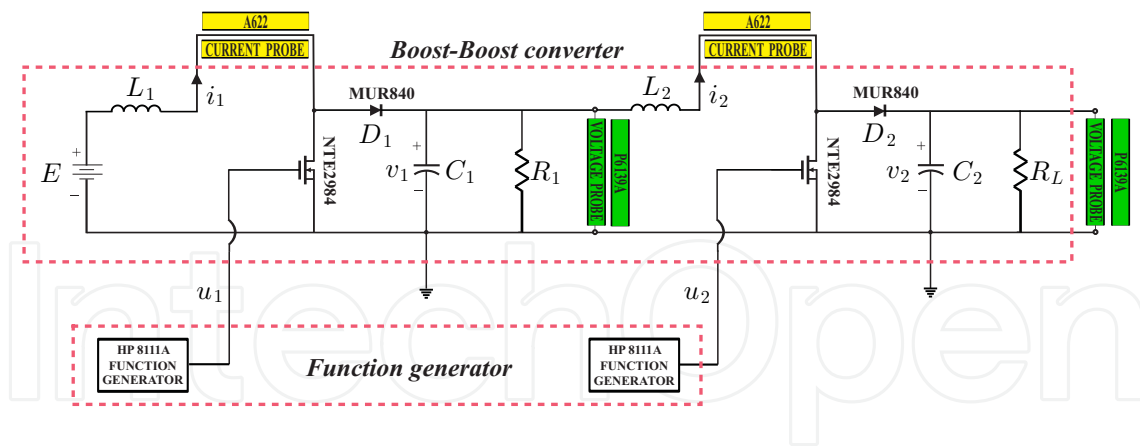


Figure 8. Electronic diagram of the Boost-Boost converter.

Since the Boost-Boost converter is integrated by two Boost converters connected in cascade, they were developed two identical printed circuit boards (PCBs) of a Boost converter that later were interconnected. The PCBs were designed by using a specialized software. In the PCBs design the inductors, transistors, and resistors were replaced by terminal blocks, this with the intent of replacing easily the components associated with the converter whenever necessary. The prototype built is shown in Figure 9.

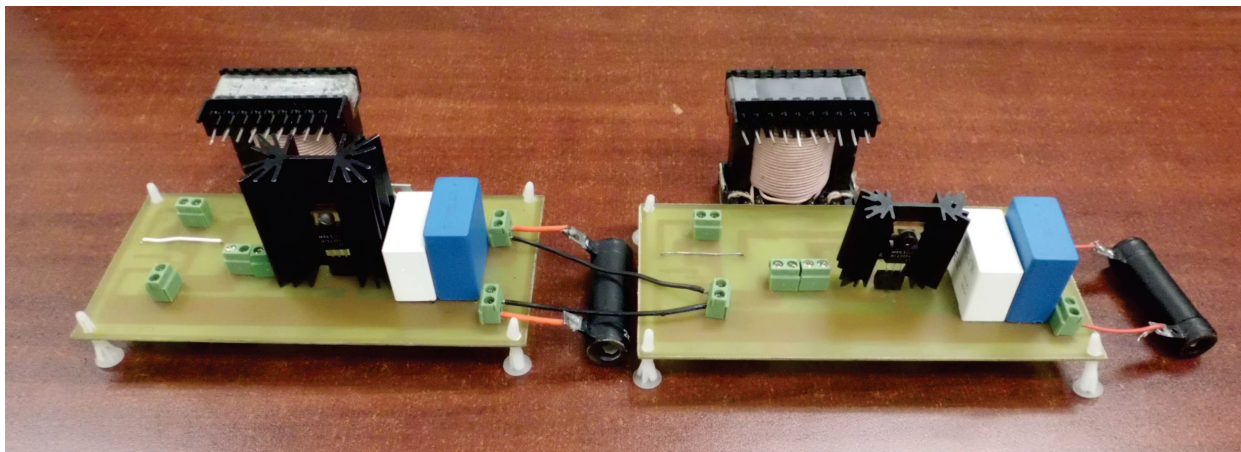


Figure 9. Boost-Boost power converter built.

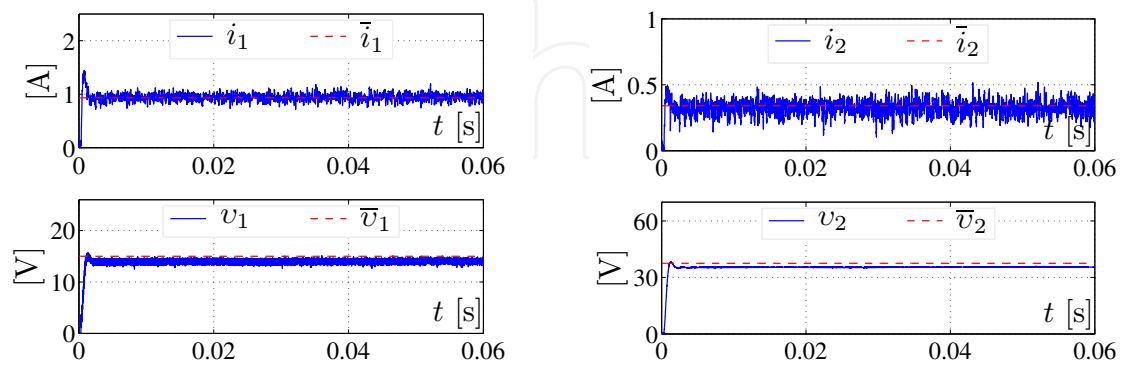
5. Experimental results

In this section the experimental results related to the dynamic responses of the converter are provided, in order to compare them with the simulation results presented in Section 3. All experiments were performed using the Boost-Boost converter described in Section 4. In order to visualize the system dynamic response Matlab/Simulink and a DS1104 electronic board from dSPACE, along with commercial current and voltage probes are employed.

5.1. Dynamic response of the converter

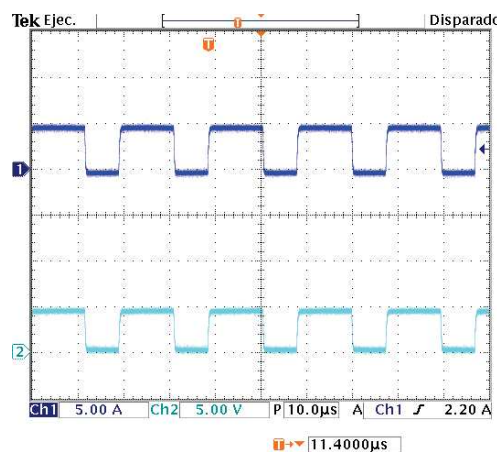
The converter dynamic response was tested experimentally for the cases indicated in Subsection 3.2.

- *Experiment I.* The experimental results associated with the *simulation I* are presented in Figure 10. These results show the dynamic response of i_1 , v_1 , i_2 , and v_2 as well as the steady-state values \bar{i}_1 , \bar{v}_1 , \bar{i}_2 , and \bar{v}_2 , respectively. Also, Figure 10 presents the input signals $u_1 = 60\%$ and $u_2 = 60\%$. The corresponding experimental numerical values measured in steady-state are $(\bar{i}_{1m}, \bar{v}_{1m}, \bar{i}_{2m}, \bar{v}_{2m}) = (930 \text{ mA}, 13.96 \text{ V}, 330 \text{ mA}, 36.95 \text{ V})$.



(a) Current through the inductor L_1 and voltage at capacitor C_1 .

(b) Current through the inductor L_2 and voltage at capacitor C_2 .



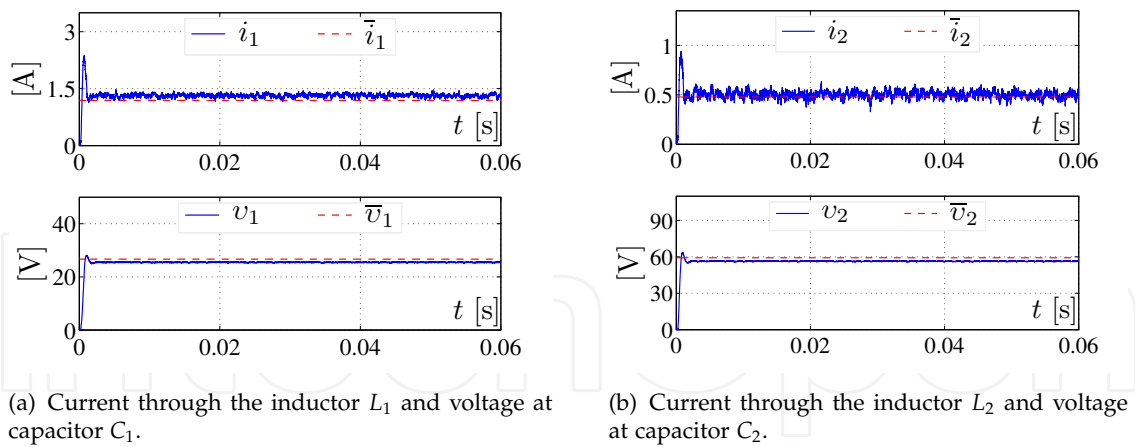
(c) Inputs $u_1 = 60\%$ (upper line) and $u_2 = 60\%$ (bottom line).

Figure 10. Dynamic response obtained from *experiment I*.

- *Experiment II.* Experimental results corresponding to *simulation II* are presented in Figure 11. Here, the experimental numerical values measured in steady-state are $(\bar{i}_{1m}, \bar{v}_{1m}, \bar{i}_{2m}, \bar{v}_{2m}) = (1.35 \text{ A}, 25.63 \text{ V}, 500 \text{ mA}, 58.5 \text{ V})$.

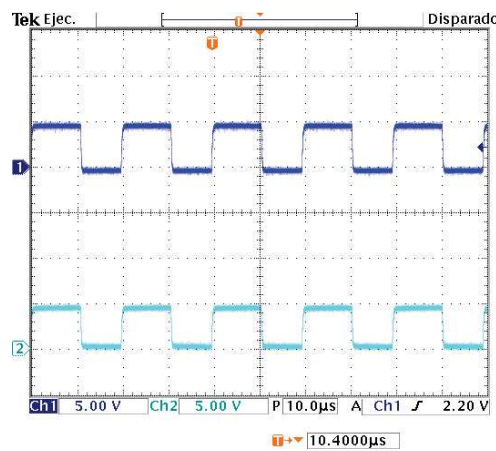
5.2. Discussion

The visualization of the converter dynamic response was accomplished via Matlab/Simulink and a DS1104 electronic board, along with current and voltage probes. The experimental results herein obtained are similar to the ones that can be obtained through the use of an oscilloscope. Although the process employed for the acquisition of the signals seems more



(a) Current through the inductor L_1 and voltage at capacitor C_1 .

(b) Current through the inductor L_2 and voltage at capacitor C_2 .



(c) Inputs $u_1 = 55\%$ (upper line) and $u_2 = 55\%$ (bottom line).

Figure 11. Dynamic response obtained from *experiment II*.

complex, the tools herein used could help in the speedy implementation of controllers in real time, in future research works, as Matlab/Simulink provides a GUI for their fast building.

Differences between simulations and experiments in the dynamic responses presented in Figures 6 and 10, on the one hand, and Figures 7 and 11, on the other, are due to the fact that the energy losses are not considered in simulations. This means that the inductors internal resistance is considered to be zero, and the semiconductor devices are assumed to be infinitely fast. Moreover, it has been shown [36] for the DC/DC Boost converter, that oscillations decrease considerably when the simulation model takes into account that the converter components are non-ideal, that is, using the Shockley diode model [37] and the Ebers-Moll transistor model [38], and taking into account the inductors internal resistance. However, it is a challenge to find a fair trade-off between complexity and accuracy; this is because to obtain better accuracy it is necessary to develop a more complex converter model. The advantage of the model used in the simulations presented in this work is simplicity and, at the same time, relatively good accuracy, which is enough for educational proposes.

6. Conclusions

In this work, a DC/DC Boost-Boost power converter was presented as a didactic material, which can be used to verify, experimentally, some theoretical concepts about electric circuit analysis studied in undergraduate courses. This work is intended to teach students how to model a practical circuit, how to design and construct, step-by-step, an experimental setup, and how use it in order to verify, experimentally, some features predicted by the model. Also, we have performed some experimental tests whose results are in accordance with predictions of the converter dynamic model. Furthermore, an additional advantage of the experimental setup is that only low-cost electronic components are employed.

Regarding the measurement and visualization of the variables involved in the converter, Matlab/Simulink, a DS1104 board, and current and voltage probes were used. These tools were employed as together they allow the system variables to be obtained easily and quickly. Moreover, Matlab/Simulink provides a graphical environment that facilitated the analysis, design and construction of the converter under study.

In future works, the Boost-Boost converter model representation based on state-space, as the one herein presented, and the acquired data in real time can be used to develop, step-by-step, different control laws. Such a procedure will be presented from design to experimental implementation, in order to accomplish the tasks of regulation and trajectory tracking associated with the converter output voltage. These tasks will be intended to teach different modern control techniques, which are generally taught at theoretical level, in the areas of electronics, electrical, automatic control, bionics, robotics, mechatronics, and so on.

Acknowledgments

R. Silva-Ortigoza and M. Marcelino-Aranda acknowledge the financial support from Secretaría de Investigación y Posgrado del Instituto Politécnico Nacional (SIP-IPN), SNI-Mexico, and the programs EDI and COFAA of IPN. The work of M. Antonio-Cruz and C. A. Merlo-Zapata was supported by CONACYT and BEIFI scholarships. Finally, G. Saldaña-González acknowledges to the Fondo Mixto CONACYT, since the publication of this work was partially supported with resources from the Fondo Mixto de Fomento a la Investigación Científica y Tecnológica CONACYT-Gobierno del Estado de Puebla.

Author details

R. Silva-Ortigoza¹, M. Antonio-Cruz¹, M. Marcelino-Aranda², G. Saldaña-González³, C. A. Merlo-Zapata¹ and P. Pérez-Romero¹

1 Instituto Politécnico Nacional. CIDETEC, Área de Mecatrónica. Unidad Profesional Adolfo López Mateos, 07700 México, DF, Mexico

2 Instituto Politécnico Nacional. UPIICSA, Sección de Estudios de Posgrado e Investigación. México, DF, Mexico

3 Universidad Tecnológica de Puebla, División de Mecatrónica, Puebla, PUE, Mexico

References

- [1] Journal Citation Reports. JCR. <http://www.webofknowledge.com/> (accessed 15 October 2013).
- [2] International Journal of Electrical Engineering Education. IJEEE. <http://www.manchesteruniversitypress.co.uk/cgi-bin/scribe?showinfo=ip023> (accessed 15 October 2013).
- [3] International Journal of Engineering Education. IJEE. <http://www.ijee.ie/> (accessed 15 October 2013).
- [4] IEEE Transactions on Education. <http://ieeexplore.ieee.org/xpl/RecentIssue.jsp?punumber=13> (accessed 15 October 2013).
- [5] Computer Applications in Engineering Education. [http://onlinelibrary.wiley.com/journal/10.1002/\(ISSN\)1099-0542](http://onlinelibrary.wiley.com/journal/10.1002/(ISSN)1099-0542) (accessed 15 October 2013).
- [6] IEEE Transactions on Learning Technologies. <http://ieeexplore.ieee.org/xpl/RecentIssue.jsp?punumber=4620076> (accessed 15 October 2013).
- [7] European Journal of Physics. EJP. <http://iopscience.iop.org/0143-0807> (accessed 15 October 2013).
- [8] American Journal of Physics. AJP. <http://ajp.aapt.org/> (accessed 15 October 2013).
- [9] Rashid MH., editor. Power Electronics Handbook. Burlington: Butterworth-Heinemann; 2011.
- [10] Mohan N., Undeland TM., Robbins WP. Power Electronics: Converters, Applications, and Design. New York: Wiley; 2003.
- [11] Sira-Ramírez H., Silva-Ortigoza R. Control Design Techniques in Power Electronics Devices. London: Springer; 2006.
- [12] Bingöl O., Paçacı S. A virtual laboratory for neural network controlled DC motors based on a DC-DC buck converter. International Journal of Engineering Education 2012;28(3) 713-723.
- [13] Silva-Ortigoza R., García-Sánchez JR., Alba-Martínez JM., Hernández-Guzmán VM., Marcelino-Aranda M., Taud H., Bautista-Quintero R. Two-Stage control design of a Buck converter/DC motor system without velocity measurements via a $\Sigma - \Delta$ modulator. Mathematical Problems in Engineering 2013; 1-11. <http://dx.doi.org/10.1155/2013/929316> (accessed 20 January 2014).
- [14] Sandoval-Ibarra F., Mercado-Moreno JR., Urióstegui-Vázquez LH. Basic circuits to design switched-based DC-DC converters. Revista Mexicana de Física 2007;53(2) 128-133.

- [15] Sandoval-Ibarra F., Mercado-Moreno JR., López A., Martínez-Rivera R., Alba-García T. Analyzing switched circuits to design DC-DC and DC-AC converters. *Revista Mexicana de Física* 2007;53(1) 1-4.
- [16] Dudrik J., Bauer P. New methods in teaching of power electronics converters and devices. *International Journal of Engineering Education* 2008;24(5) 1040-1048.
- [17] Peyović P. A new approach to the discontinuous conduction mode in switching power converters. *International Journal of Electrical Engineering Education* 2010;47(2) 168-176.
- [18] Campos-Delgado DU., Espinoza-Trejo DR. Educational experiments in power electronics and control theory: d.c. switched power supplies. *International Journal of Electrical Engineering Education* 2010;47(4) 430-447.
- [19] Altintas A. A GUI-based education toolbox for power electronics converters using MATLAB/Simulink and SimPowerSystems. *International Journal of Electrical Engineering Education* 2011;48(1) 53-65.
- [20] Abramovitz A. An approach to average modeling and simulation of switch-mode systems. *IEEE Transactions on Education* 2011;54(3) 509-517.
- [21] Deblecker O. High-resolution DPWM using sigma-delta modulator implemented on a low-cost Buck development board. *International Journal of Electrical Engineering Education* 2011;48(4) 391-404.
- [22] Zumel P., Fernández C., Sanz M., Lázaro A., Barrado A. Step-by-step design of an FPGA-based digital compensator for DC/DC converters oriented to an introductory course. *IEEE Transactions on Education* 2011;54(4) 599-609.
- [23] Liao WH., Wang SC., Liu YH. Generalized simulation model for a switched-mode power supply design course using Matlab/Simulink. *IEEE Transactions on Education* 2012;55(1) 36-47.
- [24] Lamar DG., Miaja PF., Arias M., Rodríguez A., Rodríguez M., Vázquez A., Hernando MM., Sebastián J. Experiences in the application of project-based learning in a switching-mode power supplies course. *IEEE Transactions on Education* 2012;55(1) 69-77.
- [25] Silva-Ortigoza R., Silva-Ortigoza G., Hernández-Guzmán VM., Saldaña-González G., Marcelino-Aranda M., Marciano-Melchor M. Modelling, simulation and construction of a dc/dc boost power converter: a school experimental system. *European Journal of Physics* 2012;33(3) 647-655.
- [26] Choi S., Saedifard M. An educational laboratory for digital control and rapid prototyping of power electronic circuits. *IEEE Transactions on Education* 2012;55(2) 263-270.
- [27] Middlebrook RD., Čuk S. A general unified approach to modeling switching-converter power stages. *International Journal of Electronics* 1977;42(6) 521-550.

- [28] Severns RP., Bloom GE. Modern dc-to-dc Switchmode Power Converter Circuits. New York: Van Nostrand-Reinhold; 1985.
- [29] Batarseh I. Power Electronics Circuits. New York: Wiley; 2004.
- [30] Ortega R., Loría A., Nicklasson PJ., Sira-Ramírez H. Passivity-based Control of Euler-Lagrange Systems. London: Springer-Verlag; 1998.
- [31] Hernández-Guzmán VM., Silva-Ortigoza R., Carrillo-Serrano RV. Control Automático: Teoría de Diseño, Construcción de Prototipos, Modelado, Identificación y Pruebas Experimentales. México D.F.: Colección CIDETEC-IPN; 2013. <http://controlautomatico.com.mx> (accessed 20 January 2014).
- [32] MathWorks. <http://www.mathworks.com/support/books/> (accessed 14 January 2014).
- [33] DS1104R&D Controller Board. <http://www.dspace.com/en/pub/home/products/hw/singbord/ds1104.cfm> (accessed 14 January 2014).
- [34] Karris ST. Introduction to Simulink[®] with Engineering Applications. Fremont: Orchard Publications; 2011.
- [35] Cortés-Rodríguez DJ. Generación de voltajes de CA mediante convertidores de alta frecuencia de conmutación. PhD Thesis. CICESE; 2004.
- [36] Spinetti-Rivera M. Síntesis de controladores para convertidores de potencia utilizando realimentación de la salida pasiva de la dinámica exacta del error de seguimiento: teoría y práctica. PhD thesis. Universidad Politécnica de Cataluña; 2010.
- [37] Shockley W. The theory of p-n junctions in semiconductors and p-n junction transistors. Bell System Technical Journal 1949; 28(3) 435-489.
- [38] Ebers JJ., Moll JL. Large-signal behavior of junction transistors. Institute of Radio Engineers 1954;42(12) 1761-1772.

IntechOpen

